Veronicastrum sibiricum (L.) Pennell extract alleviates inflammation-induced muscle atrophy through NLRP3 inflammasome regulation and mitochondrial function restoration

EUNHYE LEE[1], MINJEONG KWON[1] and JU-OCK NAM[1,2]

[1]School of Food Science and Biotechnology, College of Agriculture and Life Sciences, Kyungpook National University, Daegu 41566, Republic of Korea; [2]Research Institute of Tailored Food Technology, Kyungpook National University, Daegu 41566, Republic of Korea

Received January 21, 2025; Accepted July 24, 2025

DOI: 10.3892/mmr.2026.13857

Abstract. Inflammation-induced sarcopenia pathophysiology is associated with the NLR family pyrin domain containing 3 (NLRP3) inflammasome, and the concomitant mitochondrial dysfunction is a notable symptom that requires control. The *Veronicastrum* genus has anti-inflammatory and antioxidant effects; however, to the best of our knowledge, the specific mechanism associated with the seed activities and the effects on muscle have not been elucidated. Therefore, the present study aimed to evaluate how *Veronicastrum sibiricum* (L.) Pennell seed extract (VSE) can improve muscle strength under conditions of inflammation-induced muscle atrophy. The sepsis-induced sarcopenia model was used to elucidate the muscle atrophy-attenuating effects of VSE *in vitro* and *in vivo*. The mechanism of action of VSE was revealed *in vitro* by assessing the expression of associated factors at the mRNA and protein levels. Mice were administered lipopolysaccharide (LPS) intraperitoneally *in vivo* to mimic the disease state of sepsis. H&E staining was carried out to examine the cross-section of muscle tissues. ELISAs were carried out to investigate cytokine expression in mouse serum. Significant muscle atrophy was observed under the LPS-induced inflammatory state, whereas VSE decreased the expression levels of the muscle atrophy markers muscle-specific RING finger protein 1 and muscle atrophy F-box protein. Furthermore, VSE reduced the expression levels of factors involved in the NLRP3 inflammasome, such as NLRP3, GSDMD, cleaved-GSDMD, caspase-1 and cleaved-caspase-1. Additionally, the present study revealed that VSE improved mitochondrial function.

Correspondence to: Professor Ju-Ock Nam, School of Food Science and Biotechnology, College of Agriculture and Life Sciences, Kyungpook National University, 80 Daehak-ro, Buk, Daegu 41566, Republic of Korea
E-mail: namjo@knu.ac.kr

Abbreviations: LPS, lipopolysaccharide; NLRP3, NLR family pyrin domain containing 3; GSDMD, gasdermin-D; ROS, reactive oxygen species; VSE, Veronicastrum sibiricum seed extract; CCK-8, Cell Counting Kit-8; RT-qPCR, reverse transcription-quantitative PCR; GAS, gastrocnemius; TBST, Tris-buffered saline containing 0.1% Tween 20; mtROS, mitochondrial reactive oxygen species; Δψm, mitochondrial membrane potential; MuRF1, muscle-specific RING finger protein 1; MaFbx, muscle atrophy F-box protein; Nrf2, nuclear factor erythroid 2-related factor 2; HO-1, heme oxygenase-1; PGC-1α, peroxisome proliferator-activated receptor γ coactivator 1α; OXPHOS, oxidative phosphorylation system; MyHC, myosin heavy chain; ETC, electron transport chain; CoQ, coenzyme Q

Key words: sepsis, inflammation-induced muscle atrophy, NLRP3, inflammasome, translocation, mtROS

Introduction

Skeletal muscle atrophy can result from various diseases such as sepsis, cachexia, diabetes and chronic obstructive pulmonary disease, and is referred to as pathological atrophy when it occurs in these contexts (1). Increased levels of endotoxins in the bloodstream are a prevalent cause of pathological atrophy, with skeletal muscle inflammation being a key known contributing component (2,3). Lipopolysaccharide (LPS) is a representative stimulus that elicits a potent inflammatory response, leading to skeletal muscle inflammation during sepsis progression (4). Hence, clarifying the processes that govern LPS-induced inflammation in muscle is imperative.

LPS-induced sepsis is associated with muscle atrophy. Sepsis is a life-threatening condition and in severe cases, when the immune response is not properly regulated, an excessive immune response occurs, causing organ dysfunction and failure (5). The entrance of LPS into cells activates the immune system, releasing large amounts of inflammatory cytokines (such as TNF-α, IL-1β and IL-6). These cytokines activate muscle protein degradation pathways (ubiquitin-proteasome system) and inhibit protein synthesis, causing muscle wasting (6). The association between sepsis and muscle atrophy has clinical significance. Therefore, understanding the mechanisms of LPS-induced sepsis and muscle atrophy is important to maintain muscle health and develop therapeutic strategies.

Pyroptosis, a mechanism regulating cell death as an inflammatory response, is key to the development and course of sepsis (7). The activation of the NLR family pyrin domain

containing 3 (NLRP3) inflammasome initiates pyroptosis. The NLRP3 inflammasome is formed when NLRP3 receives external stimuli and activates caspase-1, which causes the pore-forming protein gasdermin-D (GSDMD) to become cleaved. The cleaved GSDMD creates pores in the cell membrane that release an overabundance of proinflammatory cytokines (such as IL-1β and IL-18), causing cell death (8,9). LPS influx is commonly recognized as triggering pyroptosis, which serves a notable role in muscle proteolysis (10). However, to the best of our knowledge, the manner in which pyroptosis mechanisms act in the healing process following inflammation-induced muscle atrophy is unknown.

Veronicastrum sibiricum (L.) Pennell is a perennial herb species that grows in northern Korea, China, Japan, Manchuria and Siberia (11). Furthermore, *Veronicastrum sibiricum* (L.) Pennell is a medicinal herb that has been previously used to treat arthritis, diarrhea and rheumatism (12). *Veronicastrum sibiricum* (L.) Pennell has been suggested to exhibit antioxidant activity by scavenging reactive oxygen species (ROS) and anti-inflammatory activity by inhibiting nitric oxide production; however, the precise mechanism of action through which *Veronicastrum sibiricum* (L.) Pennell functions remains unclear (13). Additionally, to the best of our knowledge, no prior research has been carried out on the impact of *Veronicastrum sibiricum* on muscle. There is also a dearth of research on the mechanism through which *Veronicastrum sibiricum* Pennell extract counteracts LPS-induced muscle atrophy to increase muscular strength. Therefore, the present study employed an inflammatory muscle atrophy model to investigate the mechanism of action of *Veronicastrum sibiricum* seed extract (VSE) and its impact on the pyroptosis pathway.

Materials and methods

Preparation of VSE. The VSE (cat. no. KPM012-022) used in the present study was obtained from the Natural Product Central Bank at the Korea Research Institute of Bioscience and Biotechnology. The plant was collected in 2001 from Baegam-myeon, Cheoin, Yongin Gyeonggi, Korea. To create the extract, 74 g dried and powdered seeds were added to 1 liter of 99.9% methyl alcohol (high-performance liquid chromatography grade) and extracted at room temperature through 30 cycles of ultrasonication (40 KHz; 1,500 W) for 15 min using an ultrasonic extractor (SDN-900H; Sungdong Ultrasonic Co., Ltd.), then left to stand for 120 min. The extract was filtered (Qualitative Filter No. 100; HYUNDAI MICRO Co., Ltd.) and dried under reduced pressure. A total of 6.53 g VSE was obtained.

Cell culture and differentiation. Murine C2C12 myoblast cells were obtained from American Type Culture Collection. The cells were grown at 37˚C with 5% CO_2 in DMEM (Gibco; Thermo Fisher Scientific, Inc.) with fetal bovine serum (Gibco; Thermo Fisher Scientific, Inc.) at 10% (v/v) and penicillin-streptomycin (Gibco; Thermo Fisher Scientific, Inc.) at 1% (v/v). To induce myoblast differentiation into C2C12 myotubes, once cells reached 90% confluency, the medium was switched to DMEM containing horse serum (Gibco; Thermo Fisher Scientific, Inc.) at 2% (v/v). The differentiation media were changed every 2 days and the cells were cultivated for 4 days.

Giemsa staining. C2C12 myoblasts were seeded at a concentration of $1x10^6$ cells/ml in 6-well plates and differentiated into myotubes over 4 days. Subsequently, the existing medium was removed by aspiration, and the myotubes were rinsed twice with PBS and fixed in 4% paraformaldehyde for 10 min at room temperature. Giemsa solution, diluted 1:10 in distilled water and filtered through a 0.2-μm filter, was applied to fixed cells and left for 40 min at room temperature. After removing the Giemsa solution by aspiration, cells were rinsed three times with PBS, and then imaged under a bright-field microscope (Leica Microsystems GmbH) and analyzed with ImageJ (National Institutes of Health).

Cell viability assay. Cell viability was measured using a Cell Counting Kit-8 (CCK-8; Dojindo Laboratories, Inc.) according to the manufacturer's instructions. After differentiating C2C12 myoblasts into myotubes for 4 days in 96-well plates, the cells were treated with VSE at concentrations of 0 (control), 1.25, 2.5, 5 and 10 μg/ml for 48 h at 37˚C. Given the lack of previous studies on VSE in muscle models, cytotoxicity testing was conducted to determine appropriate concentrations for subsequent experiments. After treatment, 10 μl CCK-8 solution was added to each well, and the cells were incubated for an additional 2 h. Absorbance was measured at 450 nm using a SPECTROstar microplate reader (BMG Labtech GmbH).

Reverse transcription-quantitative PCR (RT-qPCR) analysis. Total RNA was obtained from cells using RNAiso Plus Reagent (Takara Bio, Inc.). After measuring the mRNA yield, cDNA synthesis was carried out using ReverTra Ace™ qPCR RT Master Mix (cat. no. FSQ-201; Toyobo Co., Ltd.) according to the manufacturer's instructions. The reaction conditions were as follows: 37˚C for 5 min for genomic DNA removal, followed by 37˚C for 15 min for reverse transcription and 98˚C for 5 min for enzyme inactivation. RT-qPCR was performed using a Cycler iQ™ Real-Time PCR Detection System (Bio-Rad Laboratories, Inc.) and SYBR Green master mix (Toyobo Co., Ltd.) with the appropriate primers (Table I) and the template cDNA. The thermocycling conditions were as follows: Initial denaturation at 95˚C for 1 min, followed by 40 cycles of 95˚C for 15 sec and 60˚C for 60 sec. A melt curve analysis was conducted to verify amplification specificity. Analysis of relative gene expression data using RT-qPCR and the $2^{-\Delta\Delta Cq}$ method (14).

ELISA. Differentiated myotubes were pretreated with VSE at concentrations of 0 (control), 1.25, 2.5 and 5 μg/ml for 3 h at room temperature and then co-treated with LPS (500 ng/ml) for 24 h at 37˚C. Supernatants were acquired, and secretion of the proinflammatory cytokines TNF-α (cat. no. MTA00B; R&D systems, Inc.) and IL-1β was analyzed using ELISA kits (cat. no. DY401; R&D Systems, Inc.) according to the manufacturer's guidelines.

Protein extraction and western blot analysis. To acquire lysates from myotubes *in vitro*, cells were treated with 1% protease and 1% phosphatase inhibitors in RIPA buffer

Table I. Primer sequences for reverse transcription-quantitative PCR.

Gene	Primer sequence (5'-3')	
	Forward	Reverse
MuRF1	TACCAAGCCTGTGGTCATCCTG	ACGGAAACGACCTCCAGACATG
Atrogin-1	AAGGCTGTTGGAGCTGATAGCA	CACCCACATGTTAATGTTGCCC
TNF-α	TGGAACTGGCAGAAGAGGCACT	AGAGGCTCAGACATAGGCACCG
IL-1β	TGTGAAATGCCACCTTTTGA	GGTCAAAGGTTTGGAAGCAG
NLRP3	TGGACCTCTGCCGAAACTGA	CTTGAGGTGACACGTGAGGA
β-actin	CGTGCGTGACATCAAAGAGAA	GCTCGTTGCCAATAGTGATGA

NLRP3, NLR family pyrin domain containing 3; *MuRF1*, muscle-specific RING finger protein 1.

Table II. Primary antibodies used for western blotting.

Antibody	Origin	Cat. no.	Manufacturer	Dilution
Secondary antibody	Mouse monoclonal	7076	Cell Signaling Technology, Inc.	1:2,000
Secondary antibody	Rabbit monoclonal	7074	Cell Signaling Technology, Inc.	1:3,000
MyHC	Mouse monoclonal	MA5-35613	Invitrogen; Thermo Fisher Scientific, Inc.	1:1,000
MuRF1	Rabbit monoclonal	4305	Cell Signaling Technology, Inc.	1:1,000
MaFbx	Rabbit monoclonal	30919	Cell Signaling Technology, Inc.	1:1,000
Akt	Rabbit monoclonal	9272	Cell Signaling Technology, Inc.	1:1,000
p-Akt	Rabbit monoclonal	9271	Cell Signaling Technology, Inc.	1:1,000
Foxo3a	Rabbit monoclonal	2497	Cell Signaling Technology, Inc.	1:1,000
p-Foxo3a	Rabbit monoclonal	5538	Cell Signaling Technology, Inc.	1:1,000
PGC-1α	Rabbit monoclonal	ab191838	Abcam	1:1,000
OXPHOS	Mouse monoclonal	ab110413	Abcam	1:1,000
Nrf2	Rabbit monoclonal	12721	Cell Signaling Technology, Inc.	1:1,000
HO-1	Mouse monoclonal	sc-136960	Santa Cruz Biotechnology, Inc.	1:500
Keap1	Mouse monoclonal	sc-365626	Santa Cruz Biotechnology, Inc.	1:500
NLRP3	Rabbit monoclonal	15101	Cell Signaling Technology, Inc.	1:1,000
Caspase-1	Rabbit monoclonal	83383	Cell Signaling Technology, Inc.	1:1,000
Cleaved caspase-1	Rabbit monoclonal	89222	Cell Signaling Technology, Inc.	1:1,000
GSDMD	Rabbit monoclonal	39754	Cell Signaling Technology, Inc.	1:1,000
Cleaved GSDMD	Rabbit monoclonal	34677	Cell Signaling Technology, Inc.	1:1,000
β-actin	Mouse monoclonal	sc-47778	Santa Cruz Biotechnology, Inc.	1:500

MyHC, myosin heavy chain; MuRF1, muscle-specific RING finger protein 1; MaFbx, muscle atrophy F-box protein; p-, phosphorylated; PGC-1α, peroxisome proliferator-activated receptor γ coactivator 1α; OXPHOS, oxidative phosphorylation system; Nrf2, nuclear factor erythroid 2-related factor 2; HO-1, heme oxygenase-1; Keap1, kelch like ECH associated protein 1; NLRP3, NLR family pyrin domain containing 3; GSDMD, gasdermin-D.

(Biosesang) at room temperature for 30 min. To acquire lysates *in vivo*, gastrocnemius (GAS) samples were lysed using PRO-PREP™ (Intron Biotechnology, Inc.) at room temperature for 30 min. After Bradford assay quantification of protein concentrations, 30 μg of protein were separated by SDS-PAGE using 10% polyacrylamide gels. Subsequently, the proteins were transferred to a 0.2-μm nitrocellulose membrane and the membrane was blocked in 5% skimmed milk in Tris-buffered saline containing 0.1% Tween 20 (TBST) for 1 h at room temperature. Each membrane was incubated with one of 18 primary antibodies (Table II) on a shaker overnight at 4˚C to facilitate primary antibody binding. The membrane was then rinsed with TBST three times, and the membrane was incubated with secondary antibody (rabbit and mouse) at room temperature for 1 h. After rinsing three times with TBST, protein bands were detected using an enhanced chemiluminescence detection kit (Cytiva). For semi-quantitative protein expression analysis, membrane images were processed using ImageJ version 1.54d (National Institutes of Health).

Immunofluorescence assay. Myotubes were treated with either 500 ng/ml LPS alone or co-treated with 1.25, 2.5 or 5 μg/ml VSE for 24 h at 37˚C and then stained with MitoTracker Orange (Invitrogen; Thermo Fisher Scientific, Inc.) for 30 min at 37˚C. To target mitochondrial ROS (mtROS), cells were stained with MitoSOX (Invitrogen; Thermo Fisher Scientific, Inc.) dissolved in anhydrous N,N-dimethylformamide (MilliporeSigma) for 30 min at 37˚C. The mitochondria were observed at 554/576 nm, and the generation of mtROS was observed at 488/510 nm, under a fluorescence microscope. Images were recorded using the LAS X version 3.7.2.22383 software (Leica Microsystems GmbH).

To assess the mitochondrial membrane potential ($\Delta\psi$m), cells were incubated with JC-1 dye (Invitrogen; Thermo Fisher Scientific, Inc.) at a final concentration of 5 μM at 37˚C in the dark for 30 min according to the manufacturer's protocol. JC-1 fluorescence was detected at 514/529 nm for green fluorescence and 514/590 nm for red fluorescence using a fluorescence microscope (Leica Microsystems GmbH). All fluorescence intensities were quantified using ImageJ version 1.54d software (National Institutes of Health).

Animal experiments. A total of 6 male C57BL/6J mice aged 5 weeks (average body weight, 23 g) were purchased from Hyochang Science and underwent an acclimation period of 1 week. The mice were housed in an appropriately controlled environment at 25-30˚C with 50-60% relative humidity and a 12-h light/dark cycle. No restrictions were applied on access to food and water. To validate the effects of VSE in the sepsis-induced sarcopenia model, mice were divided into four groups to ensure comparable average body weights across groups with six mice per group: i) Control (saline); ii) LPS + saline (1 mg/kg LPS for 24 h); iii) LPS + low VSE (1 mg/kg LPS and 2.5 mg/kg/day VSE); and iv) LPS + high VSE (1 mg/kg LPS and 5 mg/kg/day VSE) for 7 days. LPS was dissolved in sterile water and VSE was dissolved in saline solution; all groups, including the control group, were orally administered the same volume of saline (100 μl/mouse) either alone or containing VSE daily for 7 days, followed by administration of 1 mg/kg LPS in 100 μl sterile water by intraperitoneal injection on day 8 to induce an inflammatory response *in vivo*. Body weight was measured on days 0, 2, 4, 6, 8 (before LPS treatment) and 9 (before sacrifice) to monitor the effects of VSE and LPS over time. Daily body weight measurement was avoided to minimize animal handling stress. The control group was administered sterile saline (100 μl; intraperitoneally), equivalent in volume and route to the LPS-treated group.

Grip strength tests were carried out 18 h after LPS administration. The mice were then fasted from food only, with free access to water, for 24 h in order to reduce biological variability and ensure consistency in downstream measurements. Grip strength was measured 18 h after LPS administration, based on the results of a pilot study (Fig. S1). In this study, C57BL/6J mice were intraperitoneally injected with LPS (1 mg/kg), and physiological and molecular parameters were assessed at 18 and 24 h post-injection. Body and skeletal muscle weights (gastrocnemius, tibialis anterior, extensor digitorum longus and soleus) were slightly decreased at both time points, although this was not significant. Serum TNF-α levels were significantly elevated at 18 h, and mRNA expression levels of MuRF1 and Atrogin-1 were markedly increased at 18 h compared with those in the control group (Fig. S1). Based on these results, 18 h was selected as the optimal time point for evaluating early-stage systemic inflammation and muscle atrophy. These findings support the appropriateness of the 18 h time point for grip strength measurement. Blood samples were collected and mice were sacrificed 6 h after the grip strength test. The animal experiments were approved by the Animal Ethics Committee of Kyungpook National University (approval no. KNU 2024-0511; Daegu, South Korea) and were carried out in accordance with the institution's ethical guidelines. The sample size (n=6 per group) was selected based on previous studies using murine models of inflammation-induced muscle atrophy, where similar group sizes yielded statistically valid and biologically relevant results (15-17). Additionally, the group size was determined in consideration of ethical guidelines, statistical feasibility and animal welfare. At the end of the experiment, mice were deeply anesthetized with isoflurane (4-5% in oxygen), followed by cervical dislocation. Death was confirmed by the absence of a heartbeat and corneal reflex. Immediately after sacrifice, the GAS muscles were carefully dissected, rinsed in ice-cold PBS to remove residual blood, blotted dry, snap-frozen in liquid nitrogen, and stored at -80˚C until analysis. For protein extraction, tissues were lysed in PRO-PREP™ protein extraction solution (Intron Biotechnology, Inc.) on ice, homogenized using a tissue grinder, and centrifuged at 13,000 x g for 20 min at 4˚C. The supernatants were collected and used for subsequent western blotting.

Grip strength test. Grip strengths of the mice were measured using a grip strength test device (Grip Strength Meter for Mice and Rats; Ugo Basile SRL), with five repetitions per group. After acquiring the results, the data were standardized to body weight and expressed as the mean.

H&E staining. GAS muscle tissues were obtained from each group. The tissues were fixed in 10% neutral buffered formalin at room temperature for 24 h, dehydrated and embedded in paraffin. Paraffin-embedded tissues were sectioned at a thickness of 5 μm, deparaffinized in xylene and rehydrated through a graded ethanol series followed by distilled water. The sections were then stained with hematoxylin for 5-10 min at room temperature, rinsed in water and counterstained with eosin for 1-3 min at room temperature. All staining procedures were performed using a standard protocol by a commercial pathology service (18). After staining, muscle tissue sections were imaged using a bright-light microscope, and muscle fiber organization was analyzed using ImageJ 1.54d (National Institutes of Health).

Statistical analysis. *In vitro* experiments were conducted with three independent biological replicates, and *in vivo* experiments were performed with six mice per group (n=6), and all data are presented as the mean ± SD. Statistical analyses were carried out using GraphPad Prism 9.4.1 (Dotmatics). One-way ANOVA was used to compare differences among multiple groups, followed by Tukey's post hoc test for pairwise comparisons. $P<0.05$ was considered to indicate a statistically significant difference.

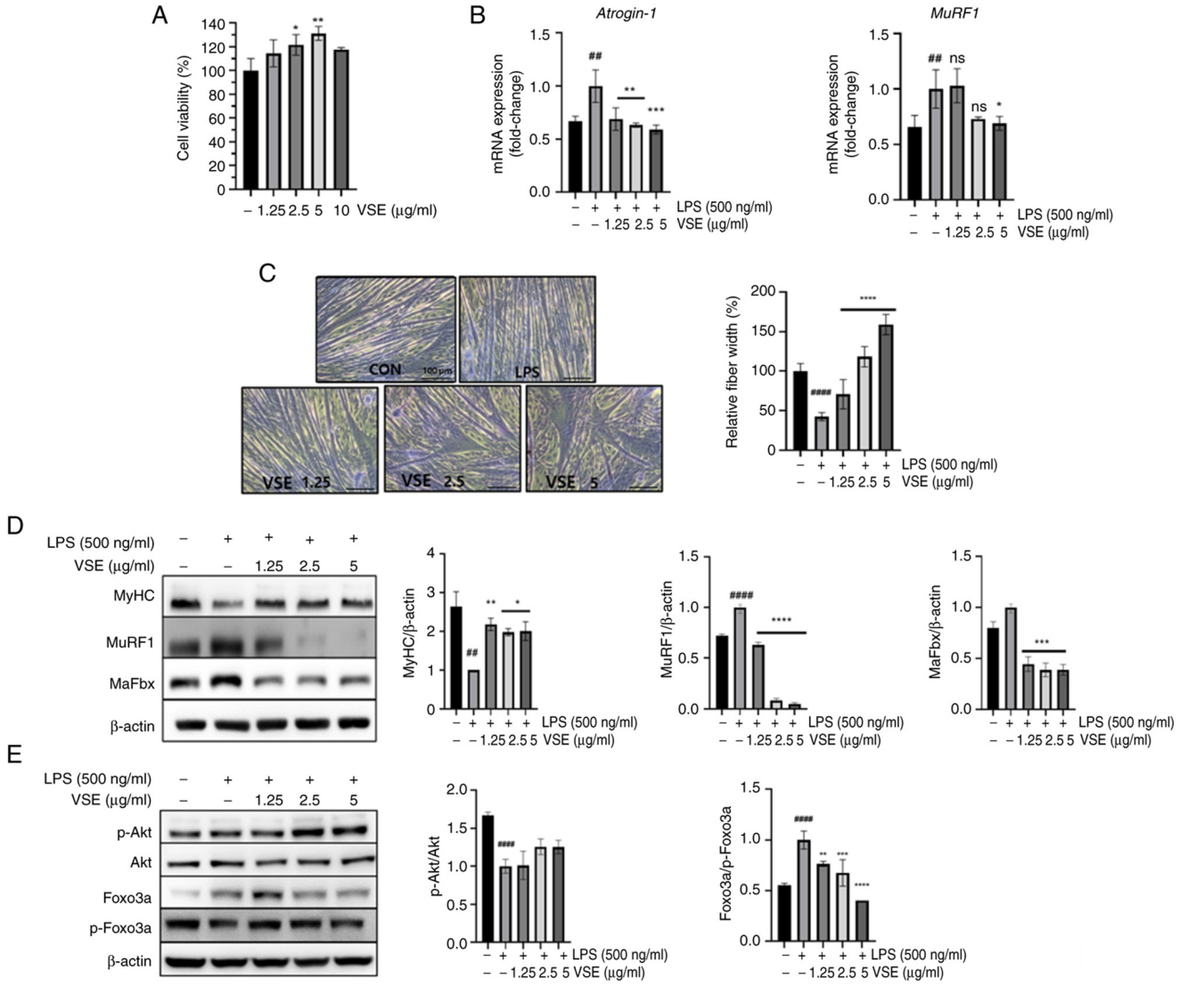

Figure 1. Effects of VSE on inflammation-induced muscle atrophy in C2C12 myotubes. All experiments were carried out after C2C12 myoblasts had differentiated into myotubes for 4 days. C2C12 myotubes were pretreated with 0 (LPS only), 1.25, 2.5 or 5 μg/ml VSE for 3 h and then co-treated with 500 ng/ml LPS for (B, D and E) 24 h and (C) 48 h. Controls received no treatments. (A) C2C12 myotubes were exposed to 0-10 μg/ml VSE for 48 h to assess cytotoxicity. (B) mRNA levels of muscle-specific E3 ubiquitin ligases *MuRF1* and *atrogin-1* were measured using reverse transcription-quantitative PCR. (C) Giemsa-stained images of C2C12 myotubes showing changes in relative fiber width after treatment. CON, untreated control; LPS, 500 ng/ml; 1.25, 2.5 and 5, co-treatment with LPS (500 ng/ml) and VSE at the indicated concentrations (μg/ml). Analysis was performed using ImageJ (National Institutes of Health). Scale bar, 100 μm. Western blot analysis of (D) MuRF1, MaFbx and MyHC protein levels, and (E) phosphorylated Akt and Foxo3a, including membrane images and semi-quantitative analysis using ImageJ. All data are presented as the mean ± SD of triplicate results and statistical analysis was carried out using one-way ANOVA with Tukey's post hoc test. $^{\#\#}$P<0.01 and $^{\#\#\#\#}$P<0.0001 vs. control group; *P<0.05, **P<0.01, ***P<0.001, ****P<0.0001 vs. LPS-treated group. MuRF1, muscle-specific RING finger protein 1; MaFbx, muscle atrophy F-box protein; MyHC, myosin heavy chain; CON, control; LPS, lipopolysaccharide; VSE, *Veronicastrum sibiricum* seed extract; p-, phosphorylated; ns, not significant.

Results

VSE attenuates inflammation-induced muscle atrophy in C2C12 myotubes. Inflammation is one of the main elements influencing skeletal muscle atrophy. Inflammation was induced in muscles using LPS, an effective proinflammatory agent (6,19). Muscle atrophy results from activation of the ubiquitin system, which is associated with muscle metabolism (20). Controlling skeletal muscle atrophy specifically requires regulation of the expression of the muscle-specific E3 ubiquitin ligases MuRF1 and muscle atrophy F-box protein (MaFbx) and their upstream mechanism, the Akt/Foxo3a pathway (21). Fig. 1 shows the effects of VSE on cell viability and muscle atrophy-related factors. As Fig. 1A illustrates, VSE exerted no toxic effects on C2C12 myotubes at concentrations ≤5 μg/ml. Meanwhile, cell viability significantly increased with VSE treatment (114-131%) compared with the non-treatment group (100%). Cell viability slightly decreased between 5 and 10 μg/ml (Fig. 1A); however, the viability at 10 μg/ml was still increased compared with the control, suggesting no cytotoxicity at concentrations >5 μg/ml. The treatment concentrations were set as 1.25, 2.5 and 5 μg/ml in subsequent experiments.

VSE treatment at 5 μg/ml reduced the upregulation of *MuRF1* and *atrogin-1* mRNA expression caused by LPS Meanwhile, an analogous pattern in expression was observed for protein expression levels of MuRF1 and MaFbx. Moreover,

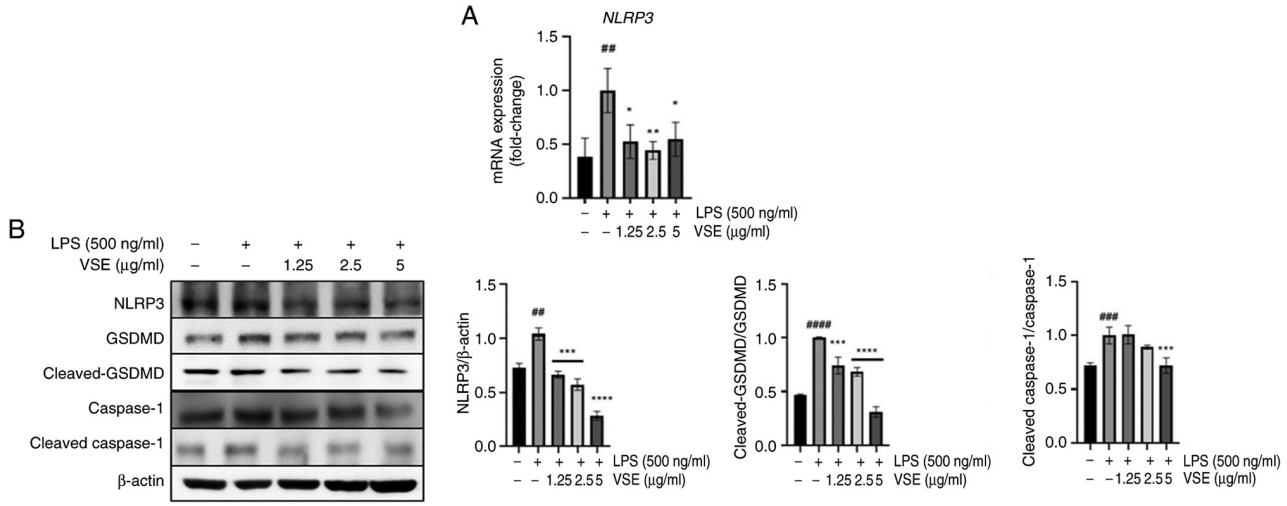

Figure 2. VSE downregulates the NLRP3 inflammasome. C2C12 myotubes were pretreated with VSE at 0 (LPS only), 1.25, 2.5 and 5 μg/ml for 3 h and then co-treated with 500 ng/ml LPS for 24 h. Controls received no treatments. (A) mRNA expression levels of *NLRP3*, the NLRP3 inflammasome initiator, were analyzed using reverse transcription-quantitative PCR. (B) Protein expression levels of factors associated with the NLPR3 pathway, a major pyroptosis pathway, were analyzed using western blotting and ImageJ. All data are presented as the mean ± SD of triplicate results and statistical analysis was carried out using one-way ANOVA with Tukey's post hoc test. $^{\#\#\#\#}$P<0.0001, $^{\#\#\#}$P<0.001, $^{\#\#}$P<0.01 vs. control; *P<0.05, **P<0.01, ***P<0.001, ****P<0.0001 vs. LPS treatment. NLRP3, NLR family pyrin domain containing 3; GSDMD, gasdermin-D; LPS, lipopolysaccharide; VSE, *Veronicastrum sibiricum* seed extract.

VSE treatment significantly attenuated the LPS-induced decrease in MyHC protein expression (Fig. 1D). Giemsa staining revealed that VSE treatment restored the thinned myotube morphology caused by LPS exposure, indicating an alleviating effect on LPS-induced atrophy (Fig. 1C). Furthermore, LPS significantly reduced the phosphorylation of both Akt and Foxo3a, leading to the activation of muscle atrophy-related genes such as *MuRF1* and *MaFbx*. By contrast, VSE treatment increased the protein levels of MyHC, phosphorylated Akt and Foxo3a (Fig. 1E). These findings indicated that VSE alleviated inflammation-induced skeletal muscle atrophy by modulating the Akt/Foxo3a signaling pathway and subsequently suppressing the expression of atrophy-related genes.

VSE mitigates pyroptosis by suppressing NLRP inflammasome activation. Pyroptosis, which is activated under various inflammatory states, including LPS-induced inflammation, is modulated by the NLRP inflammasome, with NLRP3 initiating inflammasome expression (22,23). Thus, the effect of VSE on NLRP inflammasome activation via the NLRP3 pathway was investigated (Fig. 2). When administered alone, LPS increased the mRNA levels of *NLRP3*, which were downregulated by VSE treatment to levels similar to those observed in the control group (Fig. 2A). Additionally, the protein expression levels of pyroptosis-related factors were investigated, including those of NLRP3, caspase-1, cleaved-caspase-1, GSDMD and cleaved-GSDMD. The ratios of cleaved to total caspase-1 and GSDMD were significantly increased in the LPS group, indicating activation of pyroptosis. VSE treatment effectively suppressed these ratios, suggesting inhibition of LPS-induced pyroptotic signaling. A significant reduction in cleaved caspase-1 levels was observed only for 5 μg/ml VSE (Fig. 2B). These results demonstrated that VSE may reduce NLRP3 inflammasome-mediated pyroptosis.

VSE exerts anti-inflammatory effects during pyroptosis. Release of IL-1β, a proinflammatory cytokine, is increased during pyroptosis, leading to the initiation of several cellular processes, including inflammation (24), and the release of IL-1β through cell membrane pores created by cleaved-GSDMD is considered to be a key factor in pyroptosis (25). To ascertain the effect of VSE on LPS-induced inflammatory responses, VSE-mediated release of IL-1β and TNF-α was observed. The secretion of both cytokines was evaluated at the mRNA and protein levels. When administered alone, LPS substantially increased the levels of IL-1β and TNF-α; however, VSE treatment decreased the LPS-induced upregulation at all concentrations (Fig. 3A and B). These findings suggested that the anti-inflammatory effects exerted by VSE include modifying the release of proinflammatory cytokines.

VSE alleviates oxidative stress during pyroptosis. Pyroptosis and the generation of ROS are mutually dependent, functioning as cause and effect. Specifically, regulation of mtROS is a key process in pyroptosis (26). The expression levels of factors associated with the nuclear factor erythroid 2-related factor 2 (Nrf2)/heme oxygenase-1 (HO-1) signaling pathway were assessed to examine the potential alleviating effects of VSE on oxidative stress. VSE treatment at 5 μg/ml significantly upregulated the Nrf2/HO-1 signaling pathway (Fig. 4A). Although statistical significance was not assessed, treatment with 5 μg/ml VSE appeared to increase HO-1, Nrf2 and PGC-1α expression when compared with the untreated control. Furthermore, the impact of VSE on mtROS release was assessed. To quantify this impact using immunofluorescence staining, mitotracker Orange staining, which labels mitochondria, was combined with mitoSOX green staining, specifically targeting mtROS. The LPS-induced generation of mtROS was decreased by VSE treatment (Fig. 4B), suggesting that VSE may influence pyroptosis by regulating mtROS levels.

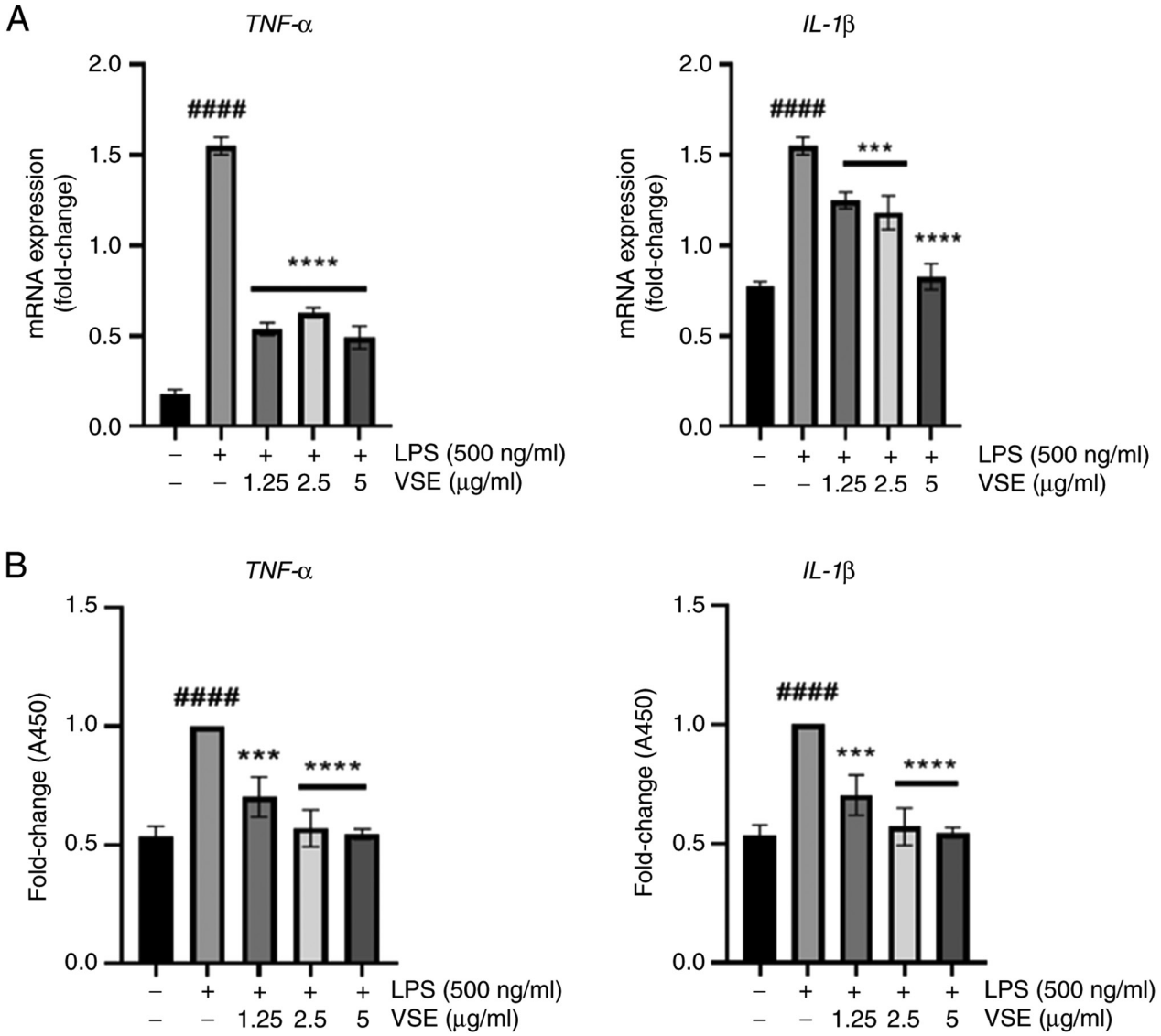

Figure 3. VSE reduces the secretion of proinflammatory cytokines. C2C12 myotubes were pretreated with VSE at 0 (LPS only), 1.25, 2.5 and 5 μg/ml for 3 h and then co-treated with 500 ng/ml LPS for 24 h. Controls received no treatments. (A) mRNA expression levels of the proinflammatory cytokines *TNF-α* and *IL-1β* were analyzed using reverse transcription-quantitative PCR. (B) Protein expression levels of the proinflammatory cytokines TNF-α and IL-1β in the supernatant of C2C12 myotube cultures were analyzed using ELISA. All data are presented as the mean ± SD of triplicate results and statistical analysis was carried out using one-way ANOVA with Tukey's post hoc test. $^{\#\#\#\#}$P<0.0001 vs. control; ***P<0.001, ****P<0.0001 vs. LPS treatment. A450, absorbance at 450 nm; LPS, lipopolysaccharide; VSE, *Veronicastrum sibiricum* seed extract.

VSE restores mitochondrial function during pyroptosis progression. The NLPR3 protein translocates to the mitochondria in response to stimuli such as LPS, which induces mitochondrial fragmentation. Healthy mitochondria are required to suppress NLPR3 inflammasome activation (27,28). Additionally, muscle atrophy is largely influenced by the degradation of mitochondrial functions, including oxidative phosphorylation, aerobic respiration and Δψm (12).

The present study aimed to investigate the effects of VSE treatment on mitochondrial functions, which are known to be negatively impacted following LPS stimulation (29). Therefore, the expression levels of oxidative phosphorylation system (OXPHOS) complexes I-V were examined. While LPS stimulation significantly reduced the expression of most OXPHOS complexes, complex IV remained unchanged. VSE treatment, however, dose-dependently restored the expression of complexes I-III and V, with complexes IV and V showing particularly notable increases at higher VSE concentrations (Fig. 5A). These findings suggest that VSE helps maintain mitochondrial metabolism at near-normal levels.

Additionally, JC-1 staining was performed to assess changes in Δψm. In healthy mitochondria, JC-1 forms aggregates emitting red fluorescence, whereas in depolarized mitochondria it exists as monomers emitting green fluorescence. LPS treatment reduced red fluorescence and significantly decreased the red/green fluorescence ratio, indicating mitochondrial depolarization. By contrast, VSE treatment restored Δψm in a dose-dependent manner, as evidenced by the increasing red/green ratio (Fig. 5B).

Collectively, these results indicate that VSE preserves mitochondrial function at both the molecular (OXPHOS protein

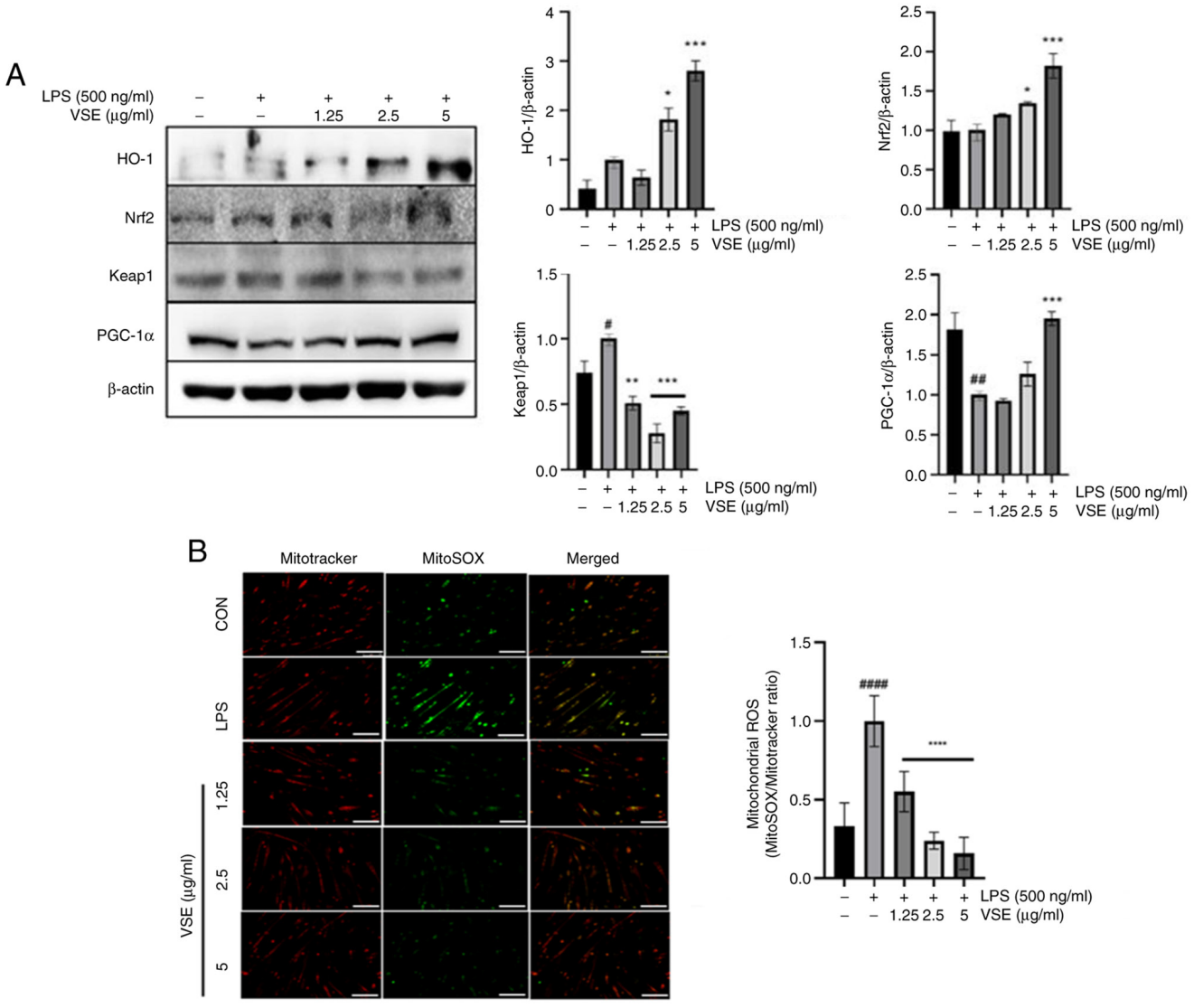

Figure 4. VSE exerts antioxidant effects in C2C12 myotubes. C2C12 myotubes were pretreated with 0 (LPS only), 1.25, 2.5 and 5 μg/ml VSE for 3 h and then co-treated with 500 ng/ml LPS for 24 h. (A) Protein expression levels of antioxidant-related factors HO-1, Nrf2 and Keap1, and mitochondrial metabolism-related factor PGC-1α were analyzed using western blotting. (B) Images (left) were obtained under a fluorescence microscope to investigate the generation of mitochondrial ROS using ImageJ (right). Scale bar, 100 μm. All data are presented as the mean ± SD of triplicate results, and statistical analysis was carried out using one-way ANOVA with Tukey's post hoc test. $^{\#}$P<0.05, $^{\#\#}$P<0.01, $^{\#\#\#\#}$P<0.0001 vs. control; *P<0.05, **P<0.01, ***P<0.001, ****P<0.0001 vs. LPS treatment. LPS, lipopolysaccharide; VSE, *Veronicastrum sibiricum* seed extract; ROS, reactive oxygen species; HO-1, heme oxygenase-1; Nrf2, nuclear factor erythroid 2-related factor 2; Keap1, kelch like ECH associated protein 1; PGC-1α, peroxisome proliferator-activated receptor γ coactivator 1α; CON, control.

expression) and functional (Δψm) levels under inflammatory conditions, potentially alleviating muscle atrophy induced by mitochondrial dysfunction.

VSE improves muscle atrophy in a sepsis-induced sarcopenia mouse model. Sepsis-induced sarcopenia is a disease in which sepsis causes a loss of muscle mass and strength; this condition is considered an important model for studying the effects of systemic inflammatory responses on muscle (30). Therefore, the potential preventive impact of VSE treatment on muscle atrophy was investigated in a sepsis-induced sarcopenia mouse model, since *in vitro* analysis revealed that VSE treatment reduced pyroptosis and muscle atrophy under LPS-induced inflammatory conditions. To this end, 2.5 and 5 mg/kg/day VSE was orally administered daily to 5-week-old male C57BL/6J mice (n=6). On the 8th day, 1 mg/kg LPS was administered intraperitoneally. Body weight was measured at specific time points (days 0, 2, 4, 6, 8 and 9). The decrease in body weight observed in all groups after day 8 can be partially attributed to pre-sacrifice fasting, while the greater reduction in the LPS group may represent LPS-induced catabolic effects. Although not statistically analyzed, VSE treatment appeared to partially restore body weight compared with the LPS group (Fig. 6A). The decrease in body weight and TA tissue weight induced by LPS was slightly restored by VSE treatment. In particular, the reduction in tissue weight caused by LPS in the tibialis anterior muscle and the recovery caused by VSE were both significant (Fig. 6B). GAS muscle tissue in the LPS-treated group comprised

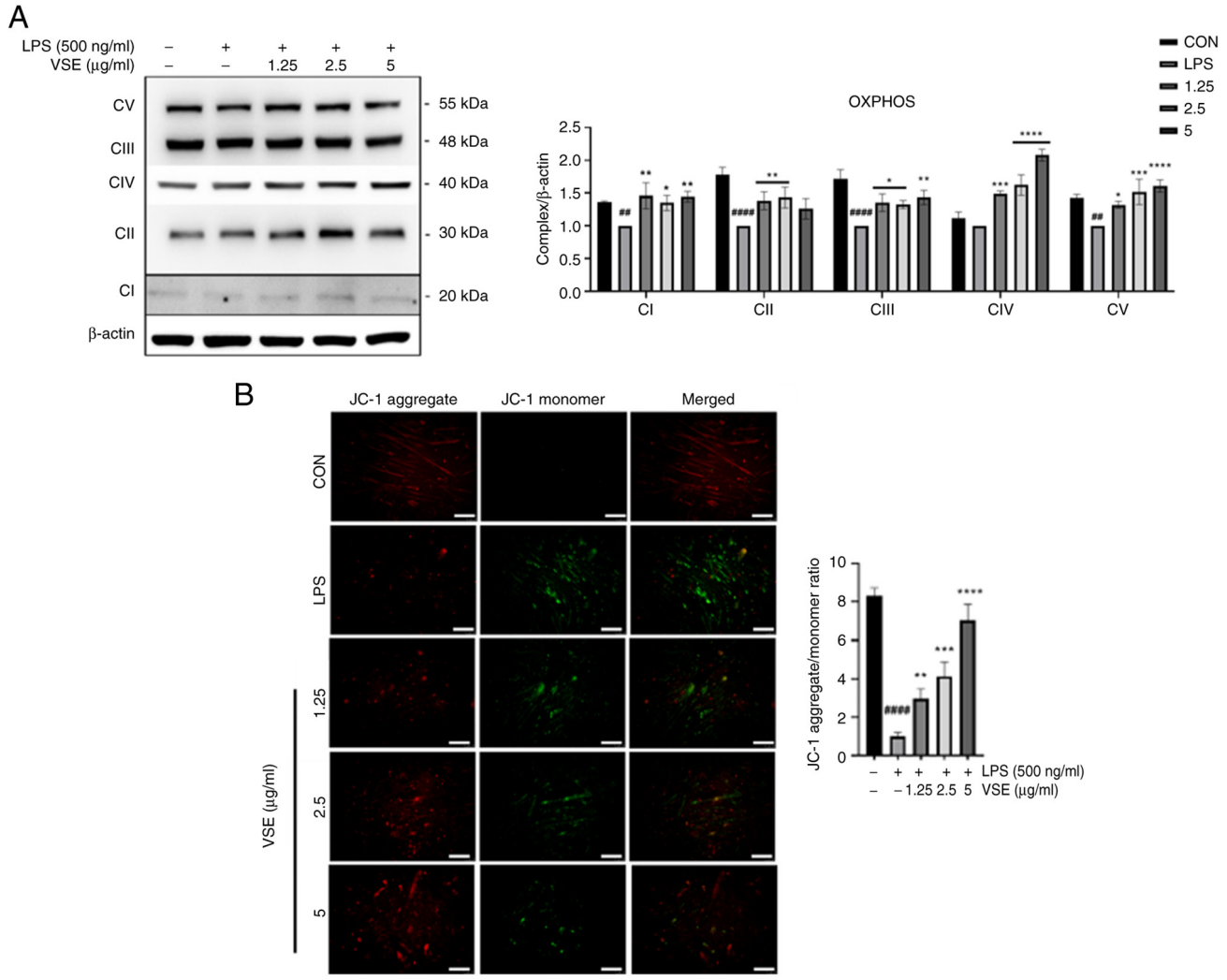

Figure 5. VSE exerts protective effects on mitochondrial function, reducing functional impairment under inflammatory conditions. C2C12 myotubes were pretreated with 0 (LPS only), 1.25, 2.5 and 5 μg/ml VSE for 3 h and then co-treated with 500 ng/ml LPS for 24 h. (A) Protein expression levels of the mitochondrial dynamics-related OXPHOS genes, including CI-CV, were analyzed using western blotting. (B) JC-1 staining was carried out to assess the mitochondrial membrane potential. Representative images of JC-1 fluorescence (red/green) were analyzed using ImageJ (National Institutes of Health). Scale bar, 25 μm. All data are presented as the mean ± SD of triplicate results and statistical analysis was carried out using one-way ANOVA with Tukey's post hoc test. $^{\#\#}$P<0.01, $^{\#\#\#\#}$P<0.0001 vs. control; *P<0.05, **P<0.01, ***P<0.001, ****P<0.0001 vs. LPS treatment. LPS, lipopolysaccharide; VSE, *Veronicastrum sibiricum* seed extract; CI-CV, complexes I-V; OXPHOS, oxidative phosphorylation system; CON, control.

very narrow fibers, and LPS treatment reduced the muscle surface area significantly. Tissue patterns were severely disrupted by LPS treatment, as evidenced by a significant reduction in muscle fiber surface area. However, VSE administration (2.5 and 5 mg/kg/day) markedly restored the tissue morphology, with the muscle fiber surface area returning to levels comparable to the control group. These improvements were confirmed by quantitative analysis using ImageJ (Fig. 6C). LPS treatment significantly weakened the grip strength of mice; however, the grip strength was significantly improved by 5 μg/ml VSE treatment (Fig. 6D). These results suggested that VSE treatment may prevent sepsis-induced sarcopenia by improving muscle strength.

VSE relieves pyroptosis in a sepsis-induced sarcopenia mouse model. NLRP3 inflammasome activation during sepsis induces muscle cell pyroptosis, a key factor in accelerating muscle fiber damage and muscle strength loss (31). Pyroptosis may also promote sarcopenia by modulating the inflammatory microenvironment within muscles (32). Similar to the *in vitro* experiments, the regulatory effects of VSE treatment on the NLRP3 inflammasome were investigated *in vivo*. The protein expression levels of the proinflammatory cytokine TNF-α were reduced in the serum of mice following VSE administration (Fig. 7A), which also reduced the mRNA expression levels of muscle degradation factor *MuRF1* in GAS tissues at 5 μg/ml of VSE (Fig. 7B). Additionally, the protein expression levels of the muscle protein degradation factors MuRF1 and MaFbx and the NLPR3 pathway-related factors NLRP3, GSDMD, cleaved-GSDMD, caspase-1 and cleaved-caspase-1 in GAS tissues were analyzed. While LPS treatment decreased myosin heavy chain (MyHC) expression, the treatment generally increased the expression levels of muscle protein degradation factors and NLRP3 pathway-related factors. Furthermore, VSE treatment restored the expression of MyHC and MafBx, and reduced the expression of MuRF1, NLRP3, cleaved-GSDMD

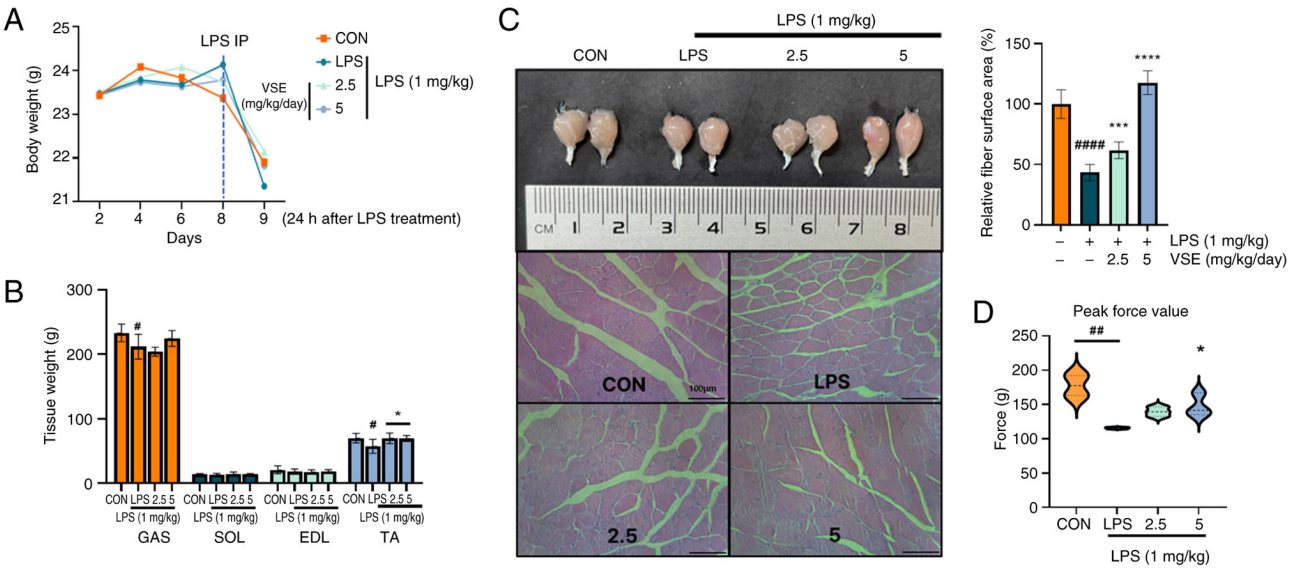

Figure 6. VSE improves muscle strength through muscle fiber recovery. (A) Body weight (n=6). (B) Muscle tissue weight of the GAS, SOL, EDL and TA muscles (n=6). (C) Images obtained after H&E staining of GAS muscle tissue. Each H&E staining image was imaged under a microscope, and the fiber surface area of the muscle tissue was quantitatively analyzed using ImageJ (National Institutes of Health). Scale bar, 100 μm. (D) Grip strength measurements (n=5 per group). All data are presented as the mean ± SD of triplicate results and statistical analysis was carried out using one-way ANOVA followed by Tukey's post hoc test in GraphPad Prism 10. $^{\#}$P<0.05, $^{\#\#}$P<0.01, $^{\#\#\#\#}$P<0.0001 vs. control; *P<0.05, ***P<0.001, ****P<0.0001 vs. LPS treatment. LPS, lipopolysaccharide; IP, intraperitoneal; VSE, *Veronicastrum sibiricum* seed extract; GAS, gastrocnemius; SOL, soleus; EDL, extensor digitorum longus; TA, tibialis anterior; CON, control.

and cleaved-caspase-1 to levels comparable with or lower than those observed in the LPS group, suggesting a protective effect against muscle atrophy and pyroptotic cell death (Fig. 7C). These results indicate that VSE may effectively counteract inflammatory muscle damage *in vivo*.

Discussion

LPS is an endotoxin, and LPS signaling is key for the pathogenesis of acute and chronic inflammatory diseases (33). In severe cases, this inflammation can lead to inflammatory myopathy and sepsis, which is characterized by skeletal muscle dysfunction due to elevations in inflammatory mediators (34). To address muscle atrophy caused by inflammation, controlling the release of inflammatory mediators by balancing anabolic and catabolic effects is potentially important (33). Anti-inflammatory medications, such as non-steroidal anti-inflammatory drugs, are actively prescribed to address inflammatory muscle atrophy; however, the prolonged use of these drugs can have adverse effects (35). One potential treatment approach is the development of natural compounds with low toxicity that specifically target inflammatory reactions (36). Ryu *et al* (37) revealed that *Sargassum Serratifolium* ethanol extract suppressed inflammation-induced muscle atrophy by exerting anti-inflammatory activity. Furthermore, Lee *et al* (38) suggested that curcumin from *Curcuma longa* L. Zingiberaceae had protective effects on sarcopenia by alleviating the inflammatory condition. Therefore, the present study aimed to investigate the potential clinical application of VSE treatment considering VSE is a phytochemical and therefore has potential in muscle wasting disorders (39).

The activation of the ubiquitin-proteasome system during an inflammatory state serves a role in muscular atrophy (1). The ubiquitin-proteasome process is activated by the interaction of three enzymes, E1, E2 and E3, and is controlled by the Akt/Foxo3a pathway, which promotes its upstream mechanism (40). Therefore, it is important to identify how the expression of E3 ligases involved in muscle atrophy is regulated. In LPS-induced inflammatory conditions, VSE treatment downregulated the protein expression levels of MaFbx and MuRF1, which are transcriptionally regulated by the Akt/Foxo3a signaling pathway. To elucidate the underlying mechanism, the upstream Akt/Foxo3a pathway was examined. Specifically, VSE increased the phosphorylation of Akt (p-Akt) and Foxo3a (p-Foxo3a), thereby suppressing the nuclear activity of Foxo3a and reducing downstream E3 ligase expression. The initiation of the NLRP3 inflammasome is regarded to be a key element in the pathogenic mechanism of pyroptosis-induced muscle atrophy (41). NLRP3 inflammasome initiation has also been demonstrated to interact with the ubiquitin-proteasome system.

Specifically, LPS can activate both canonical and non-canonical inflammasome pathways, with NLRP3 serving as a key component of the canonical pathway by sensing cellular stress and initiating caspase-1 activation (42). The NLRP3 inflammasome complex comprises the NLRP3 protein, the apoptosis-associated speck-like protein containing a caspase recruitment domain adaptor and pro-caspase-1 (43). Caspase-1 is activated following NLRP3 activation and cleaves GSDMD into cleaved GSDMD, contributing to the maturation of IL-1β. Once GSDMD is cleaved, it forms transmembrane pores that allow an excessive release of IL-1β, promoting inflammatory cell death, known as pyroptosis (44). Furthermore, numerous immune-mediated inflammatory illnesses are caused by increased IL-1β release (45). The present study aimed to elucidate the efficacy of VSE treatment in regulating factors

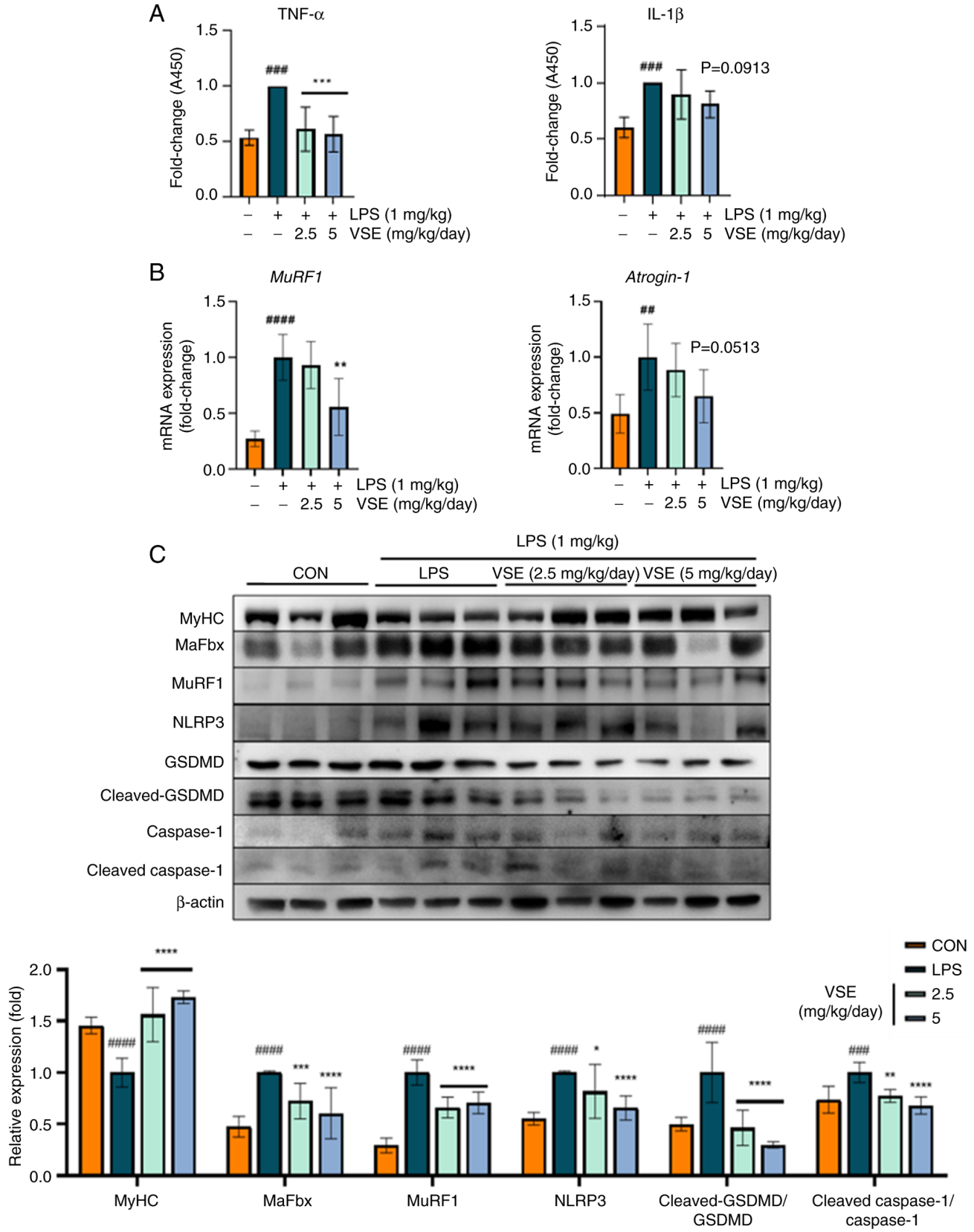

Figure 7. VSE exhibits protective effects against pyroptosis. (A) Mouse serum was obtained 24 h after intraperitoneal LPS administration, diluted to 1:50, and the protein expression levels of proinflammatory cytokines TNF-α and IL-1β were analyzed using ELISAs. (B) GAS muscle tissue was obtained, the mRNA was extracted and the mRNA expression levels of muscle atrophy-related genes *MuRF1* and *atrogin-1* were analyzed using reverse transcription-quantitative PCR. (C) GAS muscle tissue was obtained, proteins were extracted utilizing PRO-PREP™, and the protein expression levels of muscle atrophy-related and NLRP3 pathway-related proteins were analyzed using western blotting (n=6 per group). All data are presented as the mean ± SD of triplicate results and statistical analysis was carried out using one-way ANOVA followed by Tukey's post hoc test in GraphPad Prism 10. $^{\#\#}$P<0.01, $^{\#\#\#}$P<0.001, $^{\#\#\#\#}$P<0.0001 vs. control; *P<0.05, **P<0.01, ***P<0.001, ****P<0.0001 vs. LPS treatment. LPS, lipopolysaccharide; VSE, *Veronicastrum sibiricum* seed extract; GAS, gastrocnemius; MuRF1, muscle-specific RING finger protein 1; MaFbx, muscle atrophy F-box protein; MyHC, myosin heavy chain; NLRP3, NLR family pyrin domain containing 3; GSDMD, gasdermin-D; CON, control; A450, absorbance at 450 nm.

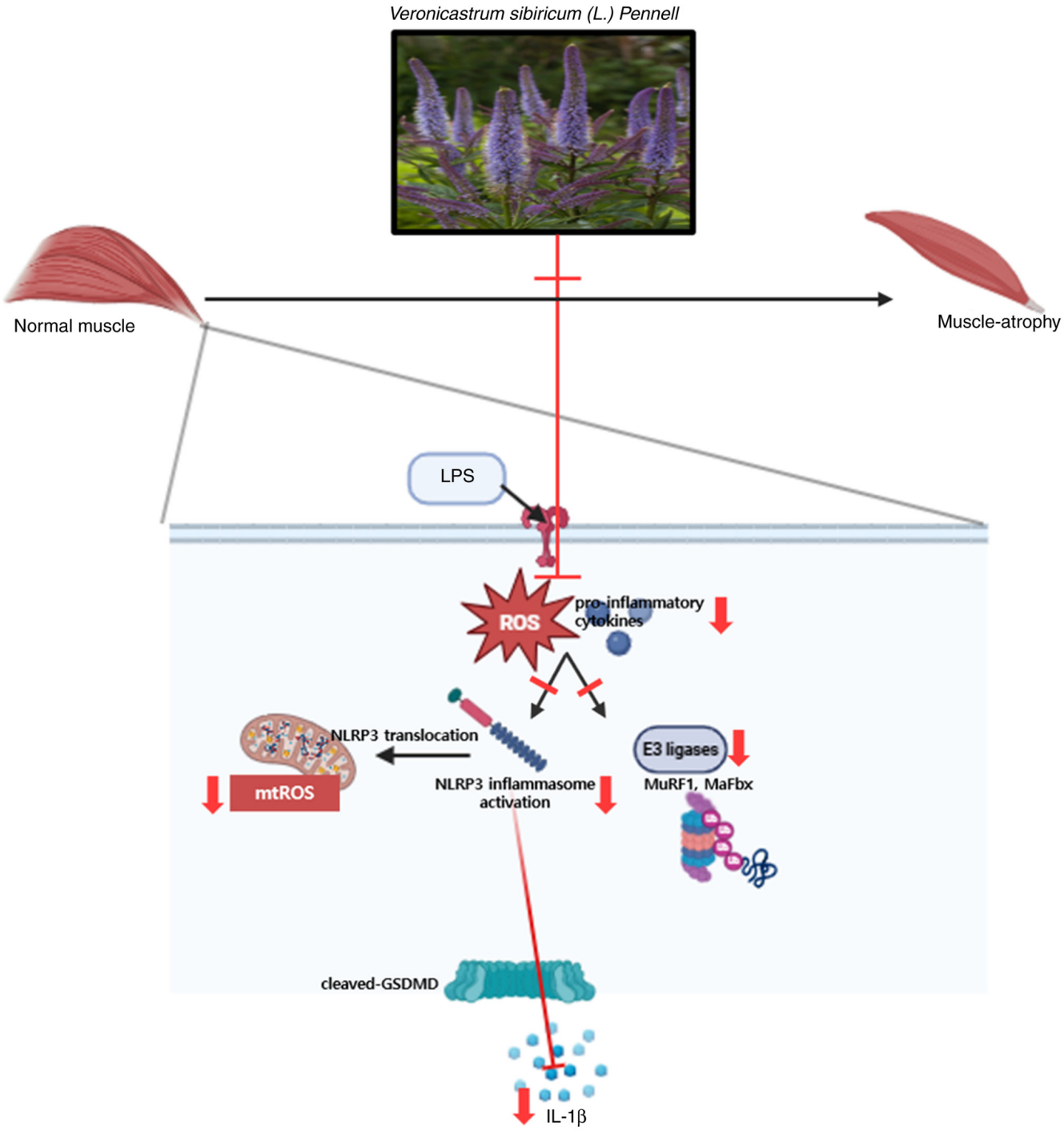

Figure 8. Schematic illustration of the VSE activation mechanism. VSE inhibits LPS-induced NLRP3 inflammasome activation and alleviates muscle atrophy through a reduction in the expression of E3 ligases. VSE, *Veronicastrum sibiricum* seed extract; LPS, lipopolysaccharide; ROS, reactive oxygen species; mtROS, mitochondrial reactive oxygen species; GSDMD, gasdermin-D; NLRP3, NLR family pyrin domain containing 3; MuRF1, muscle-specific RING finger protein 1; MaFbx, muscle atrophy F-box protein.

associated with the NLRP3 pathway, including NLRP3, caspase-1 and GSDMD. These NLRP3-associated factors were upregulated by exposure to LPS; however, VSE treatment reduced LPS-induced inflammation. Thus, the present study demonstrated that VSE may prevent cell pyroptosis by blocking NLRP inflammasome activation.

Numerous studies have reported that mitochondrial damage is inflicted by caspase-1, an NLRP3 inflammasome-associated factor, which then translocates NLRP3 to mitochondria (26,46). This phenomenon increases mtROS production, thereby impairing mitochondrial homeostasis, with high levels of damage to the inner and outer mitochondrial membranes and mitochondrial fragmentation as common symptoms (47). A previous study revealed that mtROS served a key role as a stress factor in activating the NLPR3 inflammasome (48). In addition, ATP and other NLRP3 stimulators cause an influx of Ca^{2+}, which, in turn, triggers the production of mtROS. By these mechanisms, NLRP3 inflammasome initiation and

mitochondrial dysfunction form a reciprocal network, creating a positive feedback loop (49). PGC-1α is a well-recognized element that aids in restoring mitochondrial stability, alongside being a key regulator of mitochondrial biogenesis. Increased PGC-1α expression reduces mtROS production and helps stabilize the outer and inner mitochondrial membranes (50). Upregulation of the expression of the antioxidant factors Nrf2 and HO-1 has also been revealed to aid in reducing ROS formation (51). The reduction in mtROS and the upregulation of antioxidant factors following VSE treatment in the present study suggest that VSE treatment may shield mitochondrial function against NLPR3 inflammasome activators.

OXPHOS contributes to the pivotal mitochondrial role in cellular metabolism. The primary function of this system is to control the generation of ATP (52). OXPHOS comprises five electron transport chain (ETC) complexes: CI-CV. Of these, CI is the main entry point for electrons; CII is involved in the oxidation of succinate to fumarate and transfers electrons to coenzyme Q (CoQ); and CIII, located in the center of the ETC, distributes reduced $CoQH_2$ to CIV (cytochrome *c*), which is an oxidase found outside the ETC. Finally, CV is responsible for ATP synthesis (53). Therefore, the operation of each OXPHOS complex is key to mitochondrial function. The OXPHOS system serves a major role in acute and chronic inflammation situations, meaning inhibition of the OXPHOS system accompanies a decrease in cellular function (54). The present study similarly demonstrated that mitochondrial function was impaired under LPS-induced inflammation and that VSE treatment exerted a protective effect on mitochondria, which may be explained by its capacity to increase mitochondrial function.

To further validate the protective effects of VSE on mitochondria, the Δψm was assessed using JC-1 staining, a widely used indicator of mitochondrial functional integrity (55). Under normal conditions, JC-1 accumulates in mitochondria and forms red-fluorescent aggregates, whereas in depolarized or dysfunctional mitochondria, JC-1 presents in a green-fluorescent monomeric form (56). Analysis revealed that LPS treatment reduced the red fluorescence intensity and the red/green fluorescence ratio, indicating loss of the Δψm. By contrast, VSE treatment preserved red fluorescence dose-dependently, suggesting that VSE may help maintain mitochondrial membrane integrity under inflammatory conditions. These findings further support the hypothesis that VSE alleviates mitochondrial dysfunction through structural (OXPHOS protein levels) and functional (membrane potential) recovery mechanisms.

The preventive effects of VSE on inflammatory muscle atrophy were verified by testing VSE applications in a sepsis-induced sarcopenia mouse model. The sepsis-induced sarcopenia model is suitable for evaluating muscle atrophy under inflammatory conditions (57). This muscle atrophy has clinical significance, and the sepsis model is important in understanding the pathophysiology of sarcopenia, whether occurring in acute or chronic inflammatory settings (58). The sepsis-induced sarcopenia model used in the present study was suitable for evaluating the effects of systemic inflammatory responses on muscle tissue. Furthermore, this model provided data that supported the anti-inflammatory and muscle-protective effects of VSE. In particular, VSE treatment *in vivo* downregulated mediators (NLRP3, GSDMD, cleaved-GSDMD, caspase-1 and cleaved-caspase-1) in the NLRP3 inflammasome pathway, which is known to serve a key role in sepsis-sarcopenia and fiber damage (41), supporting a possible role in attenuating sepsis-associated inflammatory responses and muscle damage.

To provide an integrated overview of the proposed mechanism, a schematic diagram is presented in Fig. 8. This illustration summarizes how VSE ameliorates LPS-induced muscle atrophy by targeting multiple key pathological events. LPS treatment induces excessive ROS production, leading to mitochondrial ROS accumulation, activation of the NLRP3 inflammasome, and the release of pro-inflammatory cytokines such as IL-1β. These changes contribute to muscle cell pyroptosis and promote the expression of muscle-specific E3 ubiquitin ligases, MuRF1 and MaFbx, thereby accelerating muscle protein degradation and fiber loss.

VSE treatment attenuates these pathological processes by suppressing mitochondrial ROS generation and inhibiting the translocation and activation of the NLRP3 inflammasome. Additionally, VSE downregulates the expression of MuRF1 and MaFbx, thereby preventing excessive muscle protein degradation. Through these combined actions, VSE effectively preserves muscle morphology and function under inflammatory conditions, supporting its therapeutic potential against inflammation-induced muscle atrophy.

Sepsis-induced sarcopenia, a severe manifestation of muscle atrophy in critically ill patients, poses pronounced clinical challenges due to its association with prolonged hospitalization, impaired physical recovery and increased mortality (59). The condition, often called intensive care unit-acquired weakness, is triggered by systemic inflammatory responses, and closely mimics the pathological features modeled in the present study (60). Therefore, the outcomes of the present research have potential translational relevance and provide valuable insights into the development of inflammation-induced sarcopenia therapeutics.

Further investigations are necessary to evaluate the full therapeutic potential of VSE. One major limitation of the present study is that the bioactive compounds within VSE have yet to be identified and characterized. While prior research has reported that plants from the *Veronicastrum* genus contain biologically active phytochemicals such as terpenoids, iridoids, flavonoids and carbohydrates, to the best of our knowledge, the specific constituents of *Veronicastrum sibiricum* seeds and their pharmacological targets remain unknown (39). Therefore, isolating and characterizing these compounds will be essential for understanding their mechanisms of action and standardizing VSE concentrations for therapeutic use. In addition, further studies should explore key physiological indicators such as the survival rate, inflammation scores and physiological states of VSE in chronic models of sarcopenia. Investigating potential synergistic effects with existing therapies and evaluating the performance of VSE in human clinical trials are also warranted to develop VSE as a novel treatment for inflammation-induced muscle atrophy.

Acknowledgements

This abstract was presented at the 2024 KFN International Symposium and Annual Meeting: Advances in Farm to Table Technologies for Human Health, held on October 23-25, 2024, at ICC JEJU, Jeju Island, Korea, and was published as Abstract no. P09-106.

Funding

No funding was received.

Availability of data and materials

The data generated in the present study may be requested from the corresponding author.

Authors' contributions

EL contributed to the design and optimization of experimental methods, data collection and performance of *in vitro* and *in vivo* experiments, statistical analysis and interpretation of results, drafting of the original manuscript, critical review and editing, validation of findings and figure preparation. MK contributed to data collection and sample preparation. JN contributed to the conception and design of experiments, performed statistical analysis and supervised the study, reviewed and edited the manuscript and managed the overall project. EL and JN confirm the authenticity of all the raw data. All authors have read and approved the final version of the manuscript.

Ethics approval and consent to participate

All animal protocols were approved by the Ethical Committee of Kyungpook National University (approval no. KNU-2024-0522; Daegu, South Korea).

Patient consent for publication

Not applicable.

Competing interests

The authors declare that they have no competing interests.

References

1. Haberecht-Müller S, Krüger E and Fielitz J: Out of control: The role of the ubiquitin proteasome system in skeletal muscle during inflammation. Biomolecules 11: 1327, 2021.
2. Zhang J, Huang Y, Chen Y, Shen X, Pan H and Yu W: Impact of muscle mass on survival in patients with sepsis: A systematic review and meta-analysis. Ann Nutr Metab 77: 330-336, 2021.
3. Valentine RJ, Jefferson MA, Kohut ML and Eo H: Imoxin attenuates LPS-induced inflammation and MuRF1 expression in mouse skeletal muscle. Physiol Rep 6: e13941, 2018.
4. Liang H, Hussey SE, Sanchez-Avila A, Tantiwong P and Musi N: Effect of lipopolysaccharide on inflammation and insulin action in human muscle. PLoS One 8: e63983, 2013.
5. Lang CH, Frost RA and Vary TC: Regulation of muscle protein synthesis during sepsis and inflammation. Am J Physiol Endocrinol Metab 293: E453-E459, 2007.
6. Frost RA, Nystrom GJ and Lang CH: Lipopolysaccharide regulates proinflammatory cytokine expression in mouse myoblasts and skeletal muscle. Am J Physiol Regul Integr Comp Physiol 283: R698-R709, 2002.
7. Bergsbaken T, Fink SL and Cookson BT: Pyroptosis: Host cell death and inflammation. Nat Rev Microbiol 7: 99-109, 2009.
8. Wang L, Jiao XF, Wu C, Li XQ, Sun HX, Shen XY, Zhang KZ, Zhao C, Liu L, Wang M, *et al*: Trimetazidine attenuates dexamethasone-induced muscle atrophy via inhibiting NLRP3/GSDMD pathway-mediated pyroptosis. Cell Death Discov 7: 251, 2021.
9. Jin H, Xie W, He M, Li H, Xiao W and Li Y: Pyroptosis and sarcopenia: Frontier perspective of disease mechanism. Cells 11: 1078, 2022.
10. Park E, Choi H, Truong CS and Jun HS: The inhibition of autophagy and pyroptosis by an ethanol extract of Nelumbo nucifera leaf contributes to the amelioration of dexamethasone-induced muscle atrophy. Nutrients 15: 804, 2023.
11. Kim MI and Kim CY: Four new acylated iridoid glycosides from the aerial part of *Veronicastrum sibiricum* and their antioxidant response element-inducing activity. Chem Biodivers 15, 2018.
12. Peng Y, Li J, Luo D, Zhang S, Li S, Wang D, Wang X, Zhang Z, Wang X, Sun C, *et al*: Muscle atrophy induced by overexpression of ALAS2 is related to muscle mitochondrial dysfunction. Skelet Muscle 11: 9, 2021.
13. Gao W, Zhang R, Jia W, Zhang J, Takaishi Y and Duan H: Immunosuppressive diterpenes from *Veronicastrum sibiricum*. Chem Pharm Bull (Tokyo) 52: 136-137, 2004.
14. Livak KJ and Schmittgen TD: Analysis of relative gene expression data using real-time quantitative PCR and the 2(-Delta Delta C(T)) method. Methods 25: 402-408, 2001.
15. Mofarrahi M, Sigala I, Guo Y, Godin R, Davis EC, Petrof B, Sandri M, Burelle Y and Hussain SN: Autophagy and skeletal muscles in sepsis. PLoS One 7: e47265, 2012.
16. Morihara N, Hino A, Miki S, Takashima M and Suzuki JI: Aged garlic extract suppresses inflammation in apolipoprotein E-knockout mice. Mol Nutr Food Res 61: 1700308, 2017.
17. Suzuki T, Kumazoe M, Kim Y, Yamashita S, Nakahara K, Tsukamoto S, Sasaki M, Hagihara T, Tsurudome Y, Huang Y, *et al*: Green tea extract containing a highly absorbent catechin prevents diet-induced lipid metabolism disorder. Sci Rep 3: 2749, 2013.
18. Fischer AH, Jacobson KA, Rose J and Zeller R: Hematoxylin and eosin staining of tissue and cell sections. CSH Protoc 2008: pdb.prot4986, 2008.
19. Ji Y, Li M, Chang M, Liu R, Qiu J, Wang K, Deng C, Shen Y, Zhu J, Wang W, *et al*: Inflammation: Roles in skeletal muscle atrophy. Antioxidants (Basel) 11: 1686, 2022.
20. Eddins MJ, Marblestone JG, Suresh Kumar KG, Leach CA, Sterner DE, Mattern MR and Nicholson B: Targeting the ubiquitin E3 ligase MuRF1 to inhibit muscle atrophy. Cell Biochem Biophys 60: 113-118, 2011.
21. Pang X, Zhang P, Chen X and Liu W: Ubiquitin-proteasome pathway in skeletal muscle atrophy. Front Physiol 14: 1289537, 2023.
22. Zhao LR, Xing RL, Wang PM, Zhang NS, Yin SJ, Li XC and Zhang L: NLRP1 and NLRP3 inflammasomes mediate LPS/ATP-induced pyroptosis in knee osteoarthritis. Mol Med Rep 17: 5463-5469, 2018.
23. Fusco R, Siracusa R, Genovese T, Cuzzocrea S and Di Paola R: Focus on the role of NLRP3 inflammasome in diseases. Int J Mol Sci 21: 4223, 2020.
24. Hsu SK, Li CY, Lin IL, Syue WJ, Chen YF, Cheng KC, Teng YN, Lin YH, Yen CH and Chiu CC: Inflammation-related pyroptosis, a novel programmed cell death pathway, and its crosstalk with immune therapy in cancer treatment. Theranostics 11: 8813-8835, 2021.
25. Li Y and Jiang Q: Uncoupled pyroptosis and IL-1β secretion downstream of inflammasome signaling. Front Immunol 14: 1128358, 2023.
26. Yu JW and Lee MS: Mitochondria and the NLRP3 inflammasome: physiological and pathological relevance. Arch Pharm Res 39: 1503-1518, 2016.
27. Nicholls DG: Mitochondrial function and dysfunction in the cell: Its relevance to aging and aging-related disease. Int J Biochem Cell Biol 34: 1372-1381, 2002.
28. Luo L, Wang F, Xu X, Ma M, Kuang G, Zhang Y, Wang D, Li W, Zhang N and Zhao K: STAT3 promotes NLRP3 inflammasome activation by mediating NLRP3 mitochondrial translocation. Exp Mol Med 56: 1980-1990, 2024.
29. Park J, Min JS, Kim B, Chae UB, Yun JW, Choi MS, Kong IK, Chang KT and Lee DS: Mitochondrial ROS govern the LPS-induced pro-inflammatory response in microglia cells by regulating MAPK and NF-κB pathways. Neurosci Lett 584: 191-196, 2015.
30. Yoshihara I, Kondo Y, Okamoto K and Tanaka H: Sepsis-associated muscle wasting: A comprehensive review from bench to bedside. Int J Mol Sci 24: 5040, 2023.
31. Liu Y, Wang D, Li T, Yang F, Li Z, Bai X and Wang Y: The role of NLRP3 inflammasome in inflammation-related skeletal muscle atrophy. Front Immunol 13: 1035709, 2022.
32. McBride MJ, Foley KP, D'Souza DM, Li YE, Lau TC, Hawke TJ and Schertzer JD: The NLRP3 inflammasome contributes to sarcopenia and lower muscle glycolytic potential in old mice. Am J Physiol Endocrinol Metab 313: E222-E232, 2017.

33. Page MJ, Kell DB and Pretorius E: The role of lipopolysaccharide-induced cell signalling in chronic inflammation. Chronic Stress (Thousand Oaks) 6: 24705470221076390, 2022.
34. Londhe P and Guttridge DC: Inflammation induced loss of skeletal muscle. Bone 80: 131-142, 2015.
35. Alturki M, Beyer I, Mets T and Bautmans I: Impact of drugs with anti-inflammatory effects on skeletal muscle and inflammation: A systematic literature review. Exp Gerontol 114: 33-49, 2018.
36. Wang RX, Zhou M, Ma HL, Qiao YB and Li QS: The role of chronic inflammation in various diseases and anti-inflammatory therapies containing natural products. ChemMedChem 16: 1576-1592, 2021.
37. Ryu H, Jeong HH, Kim MJ, Lee S, Jung WK and Lee B: Modulation of macrophage transcript and secretion profiles by *Sargassum Serratifolium* extract is associated with the suppression of muscle atrophy. Sci Rep 14: 13282, 2024.
38. Lee DY, Chun YS, Kim JK, Lee JO, Ku SK and Shim SM: Curcumin attenuates sarcopenia in chronic forced exercise executed aged mice by regulating muscle degradation and protein synthesis with antioxidant and anti-inflammatory effects. J Agric Food Chem 69: 6214-6228, 2021.
39. Mutinda ES, Mkala EM, Ren J, Kimutai F, Waswa EN, Odago WO, Nanjala C, Gichua MK, Njire MM and Hu GW: A review on the traditional uses, phytochemistry, and pharmacology of the genus Veronicastrum (Plantaginaceae). J Ethnopharmacol 300: 115695, 2023.
40. Yu H, Zhu G, Wang D, Huang X and Han F: PI3K/AKT/FOXO3a pathway induces muscle atrophy by ubiquitin-proteasome system and autophagy system in COPD rat model. Cell Biochem Biophys 82: 805-815, 2024.
41. Huang N, Kny M, Riediger F, Busch K, Schmidt S, Luft FC, Slevogt H and Fielitz J: Deletion of Nlrp3 protects from inflammation-induced skeletal muscle atrophy. Intensive Care Med Exp 5: 3, 2017.
42. Xu J and Núñez G: The NLRP3 inflammasome: Activation and regulation. Trends Biochem Sci 48: 331-344, 2023.
43. Leu WJ, Chen JC and Guh JH: Extract from plectranthus amboinicus inhibit maturation and release of interleukin 1β through inhibition of NF-κB nuclear translocation and NLRP3 inflammasome activation. Front Pharmacol 10: 573, 2019.
44. Kang L, Dai J, Wang Y, Shi P, Zou Y, Pei J, Tian Y, Zhang J, Buranasudja VC, Chen J, *et al*: Blocking caspase-1/Gsdmd and caspase-3/-8/Gsdme pyroptotic pathways rescues silicosis in mice. PLoS Genet 18: e1010515, 2022.
45. Yang Y, Wang H, Kouadir M, Song H and Shi F: Recent advances in the mechanisms of NLRP3 inflammasome activation and its inhibitors. Cell Death Dis 10: 128, 2019.
46. Wen Y, Liu Y, Tang T, Lv L, Liu H, Ma K and Liu B: NLRP3 inflammasome activation is involved in Ang II-induced kidney damage via mitochondrial dysfunction. Oncotarget 7: 54290, 2016.
47. Yu J, Nagasu H, Murakami T, Hoang H, Broderick L, Hoffman HM and Horng T: Inflammasome activation leads to caspase-1-dependent mitochondrial damage and block of mitophagy. Proc Natl Acad Sci USA 111: 15514-15519, 2014.
48. Ip WK and Medzhitov R: Macrophages monitor tissue osmolarity and induce inflammatory response through NLRP3 and NLRC4 inflammasome activation. Nat Commun 6: 6931, 2015.
49. Lee GS, Subramanian N, Kim AI, Aksentijevich I, Goldbach-Mansky R, Sacks DB, Germain RN, Kastner DL and Chae JJ: The calcium-sensing receptor regulates the NLRP3 inflammasome through Ca2+ and cAMP. Nature 492: 123-127, 2012.
50. Haque PS, Kapur N, Barrett TA and Theiss AL: Mitochondrial function and gastrointestinal diseases. Nat Rev Gastroenterol Hepatol 21: 537-555, 2024.
51. Wang X, Chen J, Tie H, Tian W, Zhao Y, Qin L, Guo S, Li Q and Bao C: Eriodictyol regulated ferroptosis, mitochondrial dysfunction, and cell viability via Nrf2/HO-1/NQO1 signaling pathway in ovarian cancer cells. J Biochem Mol Toxicol 37: e23368, 2023.
52. Putignani L, Raffa S, Pescosolido R, Aimati L, Signore F, Torrisi MR and Grammatico P: Alteration of expression levels of the oxidative phosphorylation system (OXPHOS) in breast cancer cell mitochondria. Breast Cancer Res Treat 110: 439-452, 2008.
53. Fernandez-Vizarra E and Zeviani M: Mitochondrial disorders of the OXPHOS system. FEBS Lett 595: 1062-1106, 2021.
54. Lee I and Hüttemann M: Energy crisis: The role of oxidative phosphorylation in acute inflammation and sepsis. Biochim Biophys Acta 1842: 1579-1586, 2014.
55. Smiley ST, Reers M, Mottola-Hartshorn C, Lin M, Chen A, Smith TW, Steele GD Jr and Chen LB: Intracellular heterogeneity in mitochondrial membrane potentials revealed by a J-aggregate-forming lipophilic cation JC-1. Proc Natl Acad Sci USA 88: 3671-3675, 1991.
56. Garner DL and Thomas CA: Organelle-specific probe JC-1 identifies membrane potential differences in the mitochondrial function of bovine sperm. Mol Reprod Dev 53: 222-229, 1999.
57. Goossens C, Weckx R, Derde S, Van Helleputte L, Schneidereit D, Haug M, Reischl B, Friedrich O, Van Den Bosch L, Van den Berghe G and Langouche L: Impact of prolonged sepsis on neural and muscular components of muscle contractions in a mouse model. J Cachexia Sarcopenia Muscle 12: 443-455, 2021.
58. Langhans C, Weber-Carstens S, Schmidt F, Hamati J, Kny M, Zhu X, Wollersheim T, Koch S, Krebs M, Schulz H, *et al*: Inflammation-induced acute phase response in skeletal muscle and critical illness myopathy. PLoS One 9: e92048, 2014.
59. Cox MC, Booth M, Ghita G, Wang Z, Gardner A, Hawkins RB, Darden DB, Leeuwenburgh C, Moldawer LL, Moore FA, *et al*: The impact of sarcopenia and acute muscle mass loss on long-term outcomes in critically ill patients with intra-abdominal sepsis. J Cachexia Sarcopenia Muscle 12: 1203-1213, 2021.
60. Mitobe Y, Morishita S, Ohashi K, Sakai S, Uchiyama M, Abeywickrama H, Yamada E, Kikuchi Y, Nitta M, Honda T, *et al*: Skeletal muscle index at intensive care unit admission is a predictor of intensive care unit-acquired weakness in patients with sepsis. J Clin Med Res 11: 834-841, 2019.